Manufacturing Science and Education 2025

ACTA TECHNICA NAPOCENSIS

Series: Applied Mathematics, Mechanics, and Engineering
Vol. 68, Issue Special II, Month July, 2025

A STUDY OF THE 3D PRINTING PROCESS USING A ROBOTIC ARM TO IDENTIFY THE BEHAVIOR OF PETG AND PLA MATERIALS

Florin-Daniel EDUTANU, Dragoș-Florin CHITARIU, Emilian PADURARU, Florin CHIFAN, Neculai-Eduard BUMBU, Mariana CIORAP, Cătălin Gabriel DUMITRAȘ

Abstract: *The objective of the present study is to examine the parameters employed in the robot-assisted 3D printing process. These parameters analysed include aspects such as Infill percentage, Layer thickness, and Raster angle. After the robotic 3D printing process, a test specimen is tested using standard D638-14 in a tensile testing machine, where an increasing axial force will be applied to the specimen, typically until failure, and the resulting variations will be documented. The stress/strain curve generated will demonstrate how the material reacts to the applied forces. Experiments involving robotic 3D printing with PLA and PETG materials revealed that the Ultimate Tensile Stress values for the PLA material were found to be higher than the corresponding PETG material.*
Key words*: Robot, 3D Printing, Ultimate Tensile Stress, PETG, PLA.*

1. INTRODUCTION

The field of industrial engineering is subject to constant evolution, necessitating not only innovation but also adaptation from manufacturers.

Notwithstanding these challenges, additive manufacturing represents a field that merits close observation, with forecasts indicating a substantial growth trajectory. The global additive manufacturing market is projected to reach a value exceeding $83 billion by the year 2030 [1].

The ongoing impact of 3D printing on the realm of manufacturing is indisputable, marked as it is by two principal developments, both of which are the focus of this discourse. The first is the accelerated production of intricate components, a consequence of the technology's remarkable capabilities.

The second is the concomitant reduction in material waste, an outcome that is both a by-product and a consequence of the advancements in production [2]. 3D printing with robots allows increased flexibility with large parts, planar and non-planar printing.

Most of the industry uses larger machines with robot arms that are separate from the body of the machine. These robot arms let the machine make more stuff at once, while still taking up a small amount of space.

Therefore, the benefit of robotic arm 3D printing is really noticeable when printing large objects. In these cases, the size of the object is determined by the arm's reach, rather than being limited by the fixed boundaries of a traditional 3D printer.

When printing larger parts for the car and plane industries, a robotic arm is usually used. It can have a 3D printer (FDM/FFF/FGF) or a laser/TIG welder.

A significant number of studies have analyzed 3D printing and the variation of these parameters as infill density, layer height and raster angle. However, considering the flexibility and future potential of the 3D printing process in the context of current technology, the present study proposes to determine the Ultimate Tensile Stress values for a test sample obtained from PLA and PETG materials using a robotic arm for the 3D printing process.

It is also important to note that the tensile stress produced in such a sample (and within the

elastic range of the material) results in a uniform distribution of specific stresses and strains, i.e., a homogeneous state of stresses and strains. Therefore, it can be considered the only simple stress that displays this characteristic, which explains the importance given to this tensile test of materials, due to the multitude of conclusions resulting from its performance.

2. MATERIALS AND METHODS

2.1 Materials

Two types of material, PETG and PLA, were selected for the test samples from the wide range of materials used in the 3D printing process. First, polyether ether ketone (PETG) is considered to be "one of the most easily printable materials. It is inexpensive and thus well-suited to those new to the field. Its relatively high tenacity and temperature resistance make it suitable for printing technical parts" [3]. The manufacturer provides information on the technical parameters of PETG, such as the filament diameter (1.75 mm +/- 0.02), and some of the physical properties of the filament, density (1.29 g/cm^2) and tensile modulus of wire (2,2MPa [4]. Regarding the technical specifications of Everfil PETG, the manufacturer of this type of filament recommends to use in the 3D printing process for parameters as Nozzle temperature, Table temperature and Print speed with next typical value: Nozzle temperature between 220-240°C, Table temperature between 70-90°C and Print speed between 30-60 mm/s [4].

"PETG is used universally but is especially suitable for mechanical parts for both indoor and outdoor use. PETG, it is utilized for the fabrication of components by Prusa printers" [3].

Second material, polylactic acid (PLA) is a plant-based polyester that [3]. In comparison to other materials, PLA has a number of advantages, including the fact that it does not require a heated bed, can be printed at low temperatures (with a melting point of around 175 °C) and "can be used to print both small, detailed models and large objects that fill almost the entire print volume" [3]. Regarding PLA material the manufacturer provides information on the technical parameters of PLA, such as the filament diameter (1.75 mm +/- 0.02), and some of the physical properties of the filament, like its density (1.24 g/cm2) and tensile modulus of wire (3,6 MPa) [5]. Regarding the technical specifications of Everfil PLA, the manufacturer of this type of filament recommends to use in the 3D printing process for parameters as Nozzle temperature, Table temperature and Print speed next typical value:

Nozzle temperature between 190-220 °C, Table temperature between 50-70°C and Print speed between 50-100 mm/s [5]. In the domain of industrial engineering, polyactic lactate (PLA) has been employed in the fabrication of jigs, fixtures and tools. Heineken, for instance, utilises Ultimaker Tough PLA to engineer bespoke tools for maintenance purposes [6].

2.2 Methods

Tensile Test Specimen **-** The purpose of this study is to 3D print with a robotic arm a tensile test specimen made of PETG and PLA material, testing it to determine the yield point on a stress–strain curve that indicates the limit of elasticity and an analysis of the results. Types of specimens (Type IV) and their dimensions(mm) used in own experiments is according to standard D638-14. This standard is predominantly used in the field of plastics.

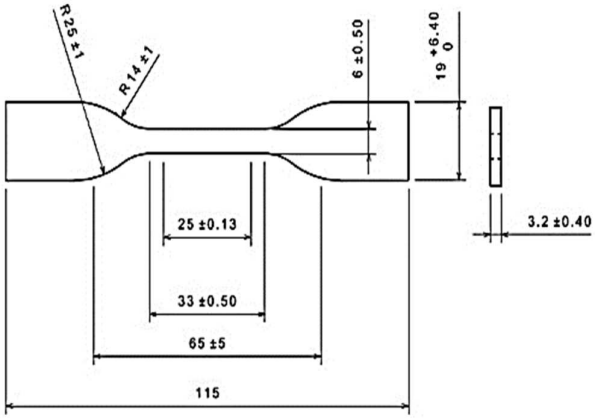

Fig. 1. Specimen Dimensions(mm) conform D638-14 [7]

During the printing procedure, the following dimensional parameters of the tensile specimen were considered, as illustrated in Figure 1. Two sets of parameters were used for our study.

In relation to the PETG material, first set of parameters includes general information of the printing process, some of which are included in

the filament manufacturer's recommendations such as nozzle temperature 230°C, bed temperature 90°C, print speed (Infill 60 mm/s, Perimeter 30mm/s, Top/Suport 60mm/s) and Infill Patterns (rectilinear for core fill pattern and top/bottom fill patern).

About PLA material, first set of parameters includes general information of the printing process, some of which are included in the filament manufacturer's recommendations such as nozzle temperature 210°C, bed temperature 70°C, print speed (Infill 90 mm/s, Perimeter 500mm/s, Top/Suport 90mm/s) and Infill Patterns (rectilinear for core fill pattern and top/bottom fill patern). Concerning to the second set of parameters, these were taken into account for the purpose of comparison with other results.

It should be noted that the study (3D printing process and tensile test specimen) was conducted at temperatures and humidity outline an optimal temperature for labs as being between 20°C and 25 °C) with humidity levels somewhere between 30% and 50%.

The subsequent step (see Table 1) involves the provision of parameters (Infill percentage (%)-IP, Layer thickness (mm)-LT, Raster angle (°)-RA) to the printer, which are comprised of three distinct types, each possessing two values (Levels).

Table 1

3D Printing Parameter.

Name	Level Number	Level Values	
IP(%)	2	60	100
LT(mm)	2	0.17	0.33
RA(°)	2	45	90

These parameters will be taken into account in a factorial experiment that will be the basis for the analysis of the data.

Equipment - The 3D and 2D models for the tensile test specimen were created using a computer-aided design (CAD) software platform. As indicated by Figure 2, the tensile test specimen was printed using a robotic arm (i.e., the Dobot Magician, model DT-MG-4R005-02E, manufactured by Shenzhen Yuejiang Technology Co., Ltd.).

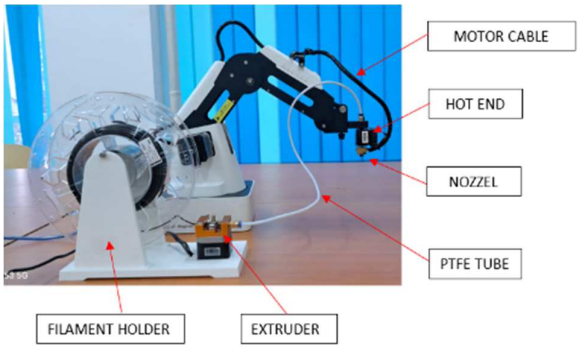

Fig. 2. Robotic Arm Dobot Magician

The robotic arm was equipped with the next components: hot end, nozzle (0.4 mm), motor cable, filament holder (located in close proximity to the robotic arm), extruder (positioned in the designated area for the filament holder), PTFE tube (connected between the extruder and the print head). The configuration of extruder parameters necessitates the utilization of 3D printing slicer software. The 3D printing function was performed with a robot arm by utilising 3D printing firmware Repetier Host V1.0.6 was employed in conjunction with a third-party program, Slic3r, which is utilised for the configuration of the 3D printer's parameters.

In order to achieve optimal results and enhance adhesion, reduce warping and curling, and enable the utilisation of a broader range of materials, the employment of a heated bed (Fig.3) is imperative. This component is an integral feature of the 3D printer, the Creality Ender-3 S1 Pro.

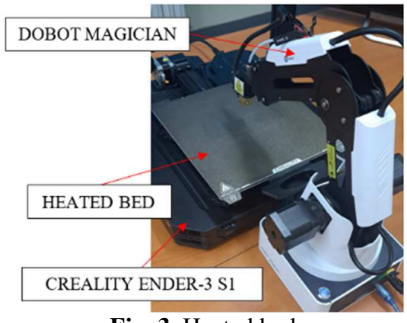

Fig. 3. Heated bed

Maintaining the heated bed and adjusting specific parameters will facilitate the production of high-quality and precise prints.

It should be noted that the 3D printing method employed in the additive manufacturing technology of the robotic arm is analogous to FDM (Fused Deposition Modelling) (see Fig. 4).

FDM functions by the deposition of "melted filament material over a build platform layer by layer, until the desired component is obtained" [8].

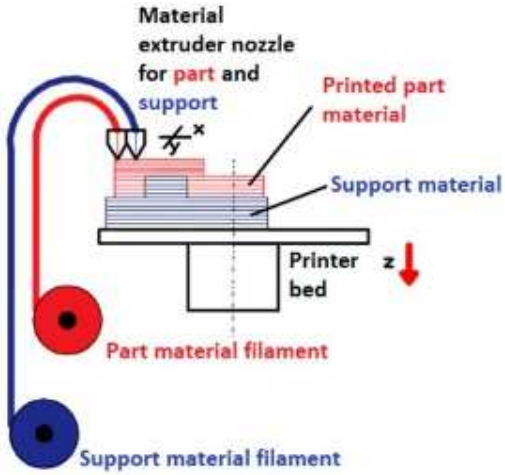

Fig. 4. Fused Deposition Modelling Process [8]

The specimen was tested using a Lloyd LRX Plus, manufacturer by Ametek Lloyd, a versatile 5kN table-top tensile tester(see Fig.5). It has an easy-to-use control panel that gives the operator all the information they need to perform simple tests. NexygenPlus v 3.0 software was used software to collect and process the results. NexygenPlus allows you to effortlessly set up tests using a graphical interface.

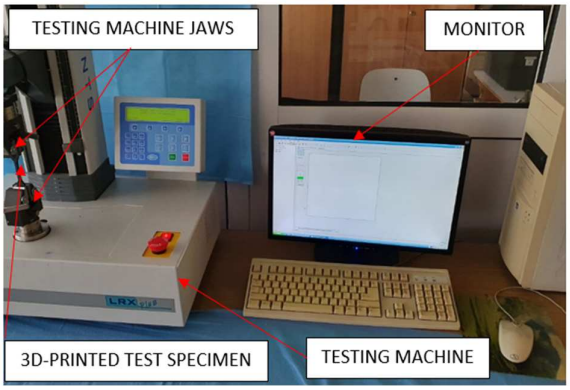

Fig. 5. Testing Equipment Lloyd LRX Plus

And the last software used in this study is Minitab, as was mention in an earlier paragraph, to analyse data. Minitab provides users with tools to perform statistical analysis, including hypothesis testing, regression analysis, and DOE.

The experiments were carried out until the point of specimen failure. The definition of failure as set out in this study is the point at which the structure is no longer able to sustain an increasing load.

The study identified distinct categories of failure in the samples examined, with the type of material influencing the occurrence of these categories (see Fig. 6). Moreover, the majority of the fracture planes demonstrate an approximate perpendicular orientation to the direction of stress.

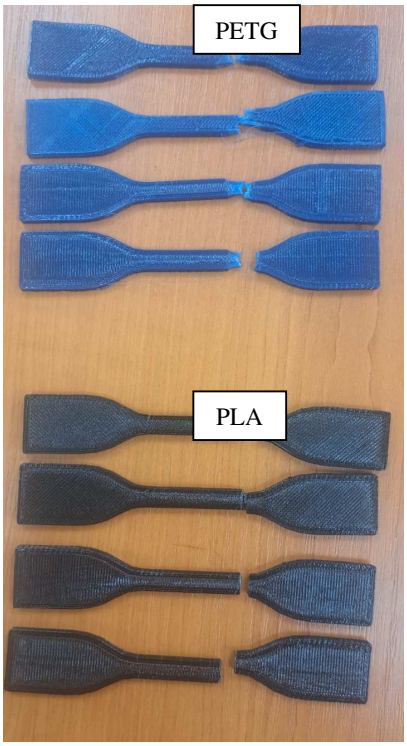

Fig.6. Failure mode for the tested 3D samples

The discrepancy between the two materials can be attributed to the mechanisms of deformation prior to fracture. Consequently, it can be deduced that PETG is more susceptible to deformation than PLA, which is a more rigid material.

Method Design of experiments via factorial designs – **"**Factorial design tests all possible conditions and works well when interactions between variables are strong and important and where every variable contributes significantly" [9]. Because factorial design can lead to a large number of trials, which can become expensive nd time-consuming, factorial design is best used for a small number of variables with few states (1 to 3). Before starting the determination, the

measurement of the force-displacement it was running Minitab software using these parameters, and a factorial experiment was performed with 2 levels and 3 factors, totaling 8 factorial design possible combinations (three factors, each of which has two levels, 2 x 2 x2 or a 2^3 =8).

The subsequent chapter will address the analysis and interpretation of the results in the context of the study's objectives and the formulated hypotheses.

3. RESULTS AND DISCUSSION

In an effort to achieve a more conclusive result, three copies were made for each of the eight specimen types, thus yielding a total of 48 specimens. The specimens were printed using two different materials, PETG (24 specimens) and PLA (24 specimens), in order to conduct a comprehensive test. It should be noted that existing standards recommend testing a minimum of five specimens. Considering the homogeneity of the results of the pre-tests of this study, it was considered sufficient to perform three test specimens, resulting in a total of 48 specimens (24 PETG, 24 PLA) as mentioned above. The ultimate tensile stress value was calculated as the average of the three samples.

In order, to determine the force-displacement curve, to comply with the test standard, the distance between the two grips of the tensile tester was set to 65 mm and the test speed to 5 mm/min at room temperature. The specimen is clamped between tensioning machine jaws, the lower one is fixed and the upper one pulls up at a constant speed and the results are shown in the form of graphs on monitor through the NexygenPlus software.

Was performed tests on the 48 specimens and the force-displacement curves were extracted. After extracting the above data on the specimens and knowing their dimensions, using the mathematical expression (1) was defined the ultimate tensile stress (σ) value, expressed in MPa.

$$\sigma = \frac{F}{A} \quad [8] \qquad (1)$$

The normal strain (ε), expressed in mm/mm, can also be determined by applying mathematical expression (2), where the displacements made by the tensile machine are known.

$$\varepsilon = \frac{\Delta L}{L} \ [8] \qquad (2)$$

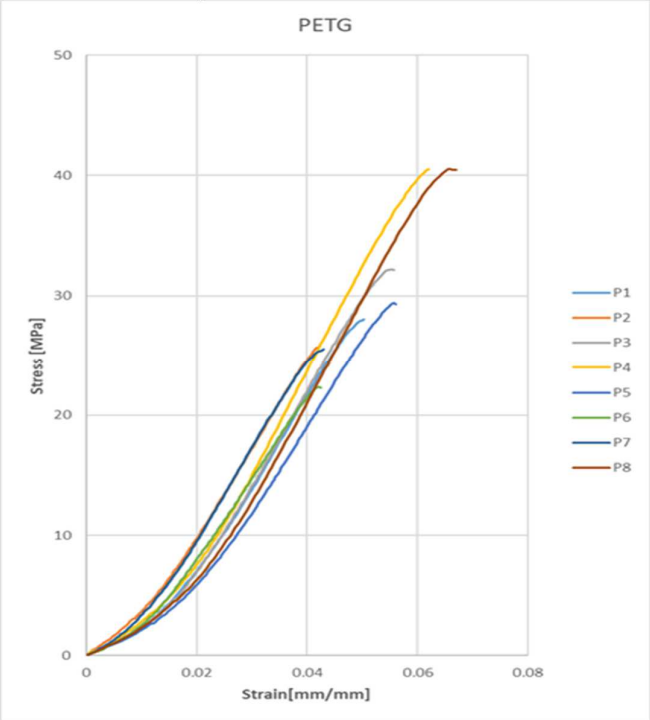

Fig.7. Stress-strain curve PETG

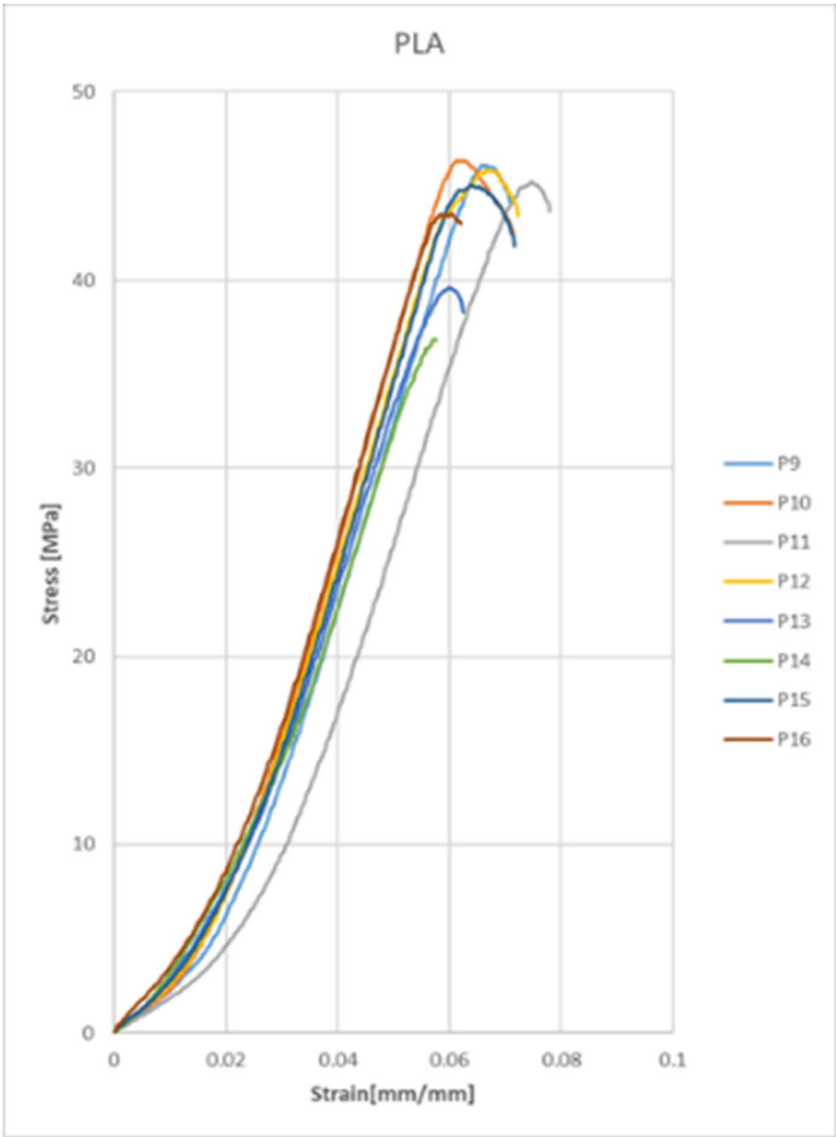

Fig.8. Stress-strain curve PLA

Therefore, after mechanical tensile testing is conducted on a given material (in our case PETG and PLA), it will exhibit different properties, among which can be mentioned its elastic modulus. "The modulus of elasticity, also known as Young's modulus (E), is therefore a measure of the stiffness of a material and is calculated using the stress-strain curves" (Fig 7,8) [10].

The following section details the printing parameters utilized by the robotic arm to obtain the PETG/PLA tensile test specimens, in conjunction with the ensuing experimental outcomes pertaining to yield points, otherwise referred to as the elastic limit (Fig.9).

Experimental results (Fig. 9) were interpreted with specialized Minitab software to create factorial, response surface, mixture is discussed below. "Interpret the key results for Analyze Factorial Design includes the Pareto chart, P-values, the Coefficients, Model Summary statistics, and the Residual Plots" [11].

In general, the Pareto Chart is a highly effective tool for demonstrating the relative importance of problems. In the present study, the Pareto chart (see Fig. 10 and Fig.11) was utilized to evaluate the magnitude and importance of the effects [12]. In the context of the Pareto chart, statistical significance is indicated by bars that intersect the reference line. In the context of our study, the bars representing factors such as infill percentage (%), layer thickness (mm), and raster angle (°) did not intersect the reference line, which is set at 2.776.

Material	Run Order	IP (%)	LT(mm)	RA(°)	Yield Stress (MPa)
PETG	P1	60	0.17	45	29.38
	P2	60	0.33	45	28.03
	P3	100	0.17	45	25.53
	P4	100	0.17	90	40.54
	P5	100	0.33	45	32.23
	P6	60	0.33	90	25.84
	P7	100	0.33	90	40.53
	P8	60	0.17	90	24.17
PLA	P9	60	0.17	45	39.63
	P10	100	0.17	45	45.03
	P11	60	0.33	90	46.35
	P12	60	0.17	90	36.9
	P13	100	0.33	45	45.2
	P14	100	0.17	90	43.8
	P15	60	0.33	45	46.12
	P16	100	0.33	90	45.86

Fig.9. 3D Printing parameter and ultimate tensile stress value

Experimental results (Fig. 9) were interpreted with specialized Minitab software to create factorial, response surface, mixture is discussed below. “Interpret the key results for Analyze Factorial Design includes the Pareto chart, P-values, the Coefficients, Model Summary statistics, and the Residual Plots” [11].

In general, the Pareto Chart is a highly effective tool for demonstrating the relative importance of problems. In the present study, the Pareto chart (see Fig. 10 and Fig.11) was utilized to evaluate the magnitude and importance of the effects [12]. In the context of the Pareto chart, statistical significance is indicated by bars that intersect the reference line. In the context of our study, the bars representing factors such as infill percentage (%), layer thickness (mm), and raster angle (°) did not intersect the reference line, which is set at 2.776.

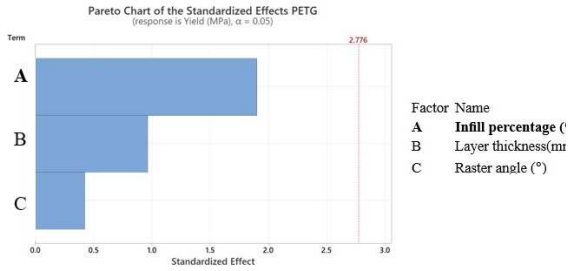

Fig.10. Pareto Chart of the Standardized Effects PETG

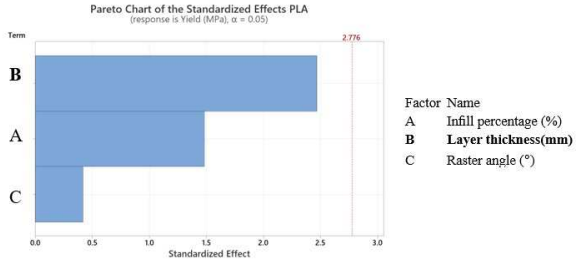

Fig.11. Pareto Chart of the Standardized Effects PLA

It is important to note that even in the event of encountering a significant factor, the Pareto chart displays only the absolute value of the effects.

In order to “determine the statistical significance of the association between the response and each term in the model, it is necessary to compare the P-value for the term to the designated significance level” [13] [11].

This process enables the assessment of the null hypothesis, which postulates that the term's coefficient is equivalent to zero. This hypothesis suggests the absence of an association between the term and the response.

Typically, a significance level (denoted as α or alpha) of 0.05 is considered adequate for this purpose. This is because a significance level of 0.05 indicates a 5% risk of concluding that an association exists when there is no actual association.

Analysis of variance (ANOVA) is a pivotal statistical instrument utilised within the domain of design of experiments (DOE) to ascertain which factors have a significant impact on a response variable.

According to the results displayed in Fig.12 and Fig.13 the P-value exceeds alpha, indicating a lack of statistically significant association between the response variable and the term under investigation – Robotic 3D printing parameters infill percentage (%), layer thickness (mm), and raster angle (°).

Analysis of Variance PETG					
Source	DF	Adj SS	Adj MS	F-Value	P-Value
Model	3	161.11	53.70	1.57	0.33
Linear	3	161.11	53.70	1.57	0.33
Infill percentage (%)	1	123.32	123.32	3.61	0.13
Layer thickness(mm)	1	6.14	6.14	0.18	0.69
Raster angle (°)	1	31.64	31.64	0.93	0.39
Error	4	136.50	34.12		
Total	7	297.60			

Fig.12. Analysis of Variance PETG

Analysis of Variance PLA					
Source	DF	Adj SS	Adj MS	F-Value	P-Value
Model	3	57.271	19.09	2.82	0.171
Linear	3	57.271	19.09	2.82	0.171
Infill percentage(%)	1	14.824	14.824	2.19	0.213
Layer thickness(mm)	1	41.269	41.269	6.1	0.069
Raster angle(°)	1	1.178	1.178	0.17	0.698
Error	4	27.045	6.761		
Total	7	84.315			

Fig.13. Analysis of Variance PETG

A model summary table is "a tool that is used to assess the quality of the model's fit to the data and examine the goodness-of-fit statistics" (Fig.14) [14] [11].

Model Summary				
Material	S	R-sq	R-sq(adj)	R-sq(pred)
PETG	5.84158	54.13%	19.74%	0.00%
PLA	2.60022	67.92%	43.87%	0.00%

Fig.14. Model Summary

The model accounts for 54.13%(PETG)/ 67.92%(PLA) of the variance of the factors involved, as indicated by this result. The literature suggests that obtaining a higher R-sq value would allow for a more precise fit of the model to the hypothesized data. The R-sq value typically ranges from 0% to 100%. In this instance, the R-sq value indicates that the model provides a slightly above-average fit to the selected data.

In the present model, the value of R-sq(adj) does not include the number of predictors that seem to lead to a recommended model selection. Given its well-documented predilection to underperform, it is advisable to augment the R-sq(adj) value.

Finally, an analysis is conducted to determine whether the selected model fulfils the hypotheses of the analysis.

Residual plots are utilized to assess the model's appropriateness and to ascertain whether it satisfies the assumptions of the analysis (graphical method of checking the degree of correlation between a model's predictions and actual data).

A "Histogram's" efficacy is optimal when the data set contains approximately 20 or more data points [11]. In our case of a small sample size, each bar on the histogram contains an insufficient number of data points to reliably show skewness or outliers.

The "Normal probability plot of the residuals is employed to assess the hypothesis that the residuals are normally distributed" [11]. In general, the normal probability plot of the residuals should approximate a straight line, as is evident in the case of our study. Consequently, our model exhibits tendencies to fulfill the assumptions made in its realization. It is characterized by an absence of distinctive attributes, such as nonlinearity, points that deviate from the reference line, or an altered gradient.

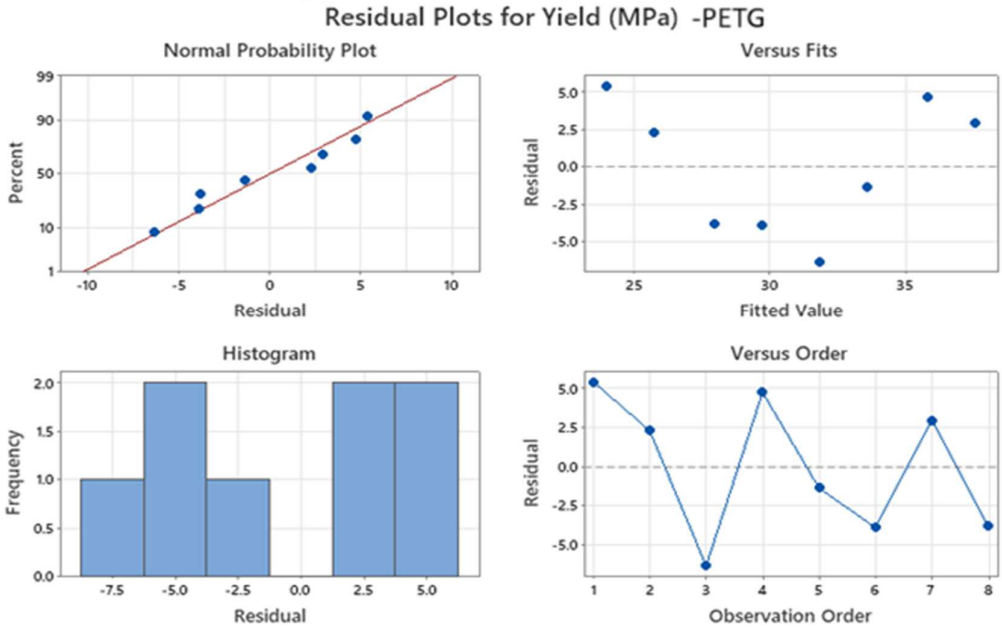

Fig.15. Residual plots for Ultimate Tensile Stress PETG

The "Residuals versus fits plot graph, Fig.15 and Fig.16, is a graphical representation used to verify the assumption that the residuals are randomly distributed and have constant variance" [15] [11]. Ideally, the points should fall randomly on both sides of 0, with no recognizable patterns in the points. In our case, residuals are mostly positive when the fitted value is small, negative when the fitted value is in the middle, and positive when the fitted value is large. The hypothesis that residuals are independent of each other can be tested using the plot of "Residuals versus order". Independent residuals demonstrate no trends or patterns when displayed in time order. However, the presence of patterns in dots may indicate that residues close to each other may be correlated and therefore not independent.

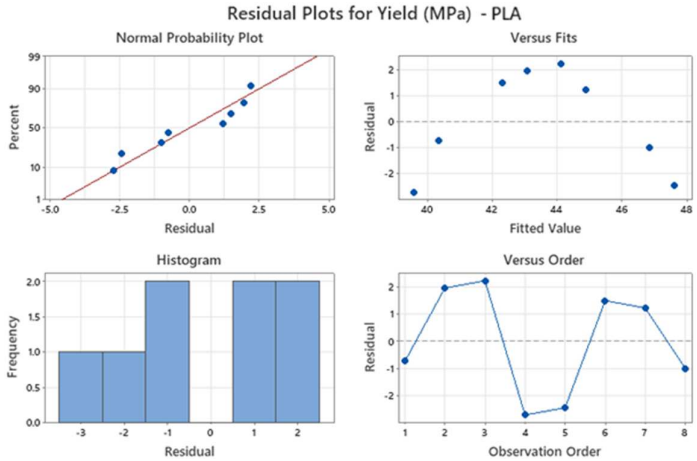

Fig.16. Residual plots for Ultimate Tensile Stress PLA

The utilization of interaction plots is integral to the evaluation of two-way interactions. The assessment of lines is predicated on a comprehensive understanding of how these interactions affect the response [16], [11]. The graph displays a full interaction plot matrix, with each pair of variables providing two panels, as summarized below in Fig.17 and Fig.18.

In the case of the PETG and PLA materials used to create the test specimen the following observations can be made:

- Row 1/2/3 panel: A comparison of the results obtained for these two materials, utilising identical parameters, proves that the lack of interaction between "Infill Percentage" and "Layer Thickness", "Infill Percentage" and "Raster Angle", "Layer Thickness" and "Raster Angle" and suggests that each pair of factors are not significantly important for PETG material and that they are also unlikely to be significantly important for PLA.

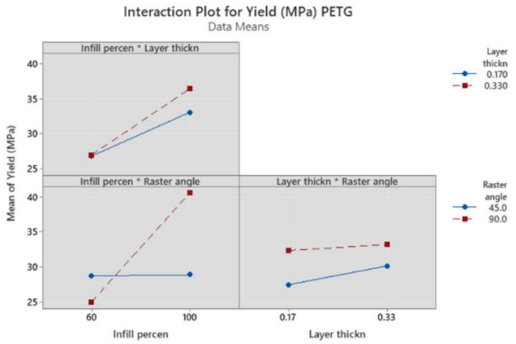

Fig.17. Interaction Plot for Ultimate Tensile Stress (MPa) PETG

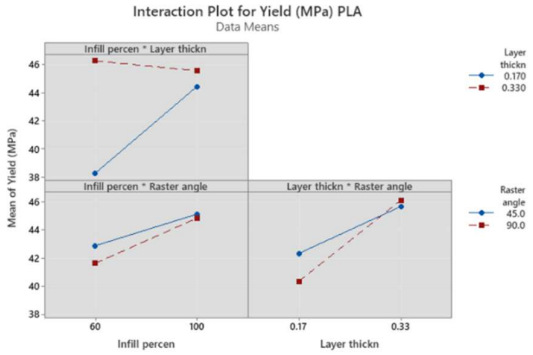

Fig.18. Interaction Plot for Ultimate Tensile Stress (MPa) PLA

Also, these results demonstrated how the parameters interact bidirectional and how this affects the Ultimate Tensile Stress (MPa).

This showed that the apparent effects of this interaction were caused by the non-parallel nature of the lines and consequently indicates that the relationship between the Ultimate Tensile Stress (MPa) and each factor depends on the setting of another factor.

The Main Effects Plot constitutes a graphical instrument utilised within the domain of Design of Experiments (DOE), with the purpose of visually evaluating the impact of varying factors on a response variable

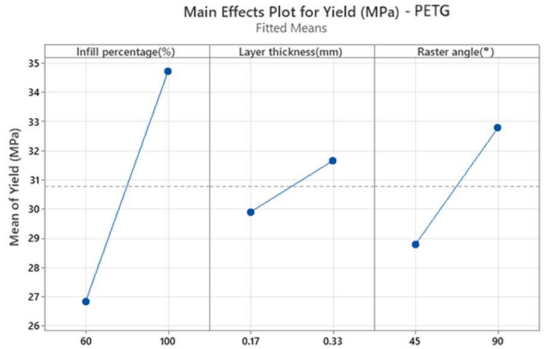

Fig.19. Main Effects Plot for Yield Ultimate Tensile Stress (MPa) PETG

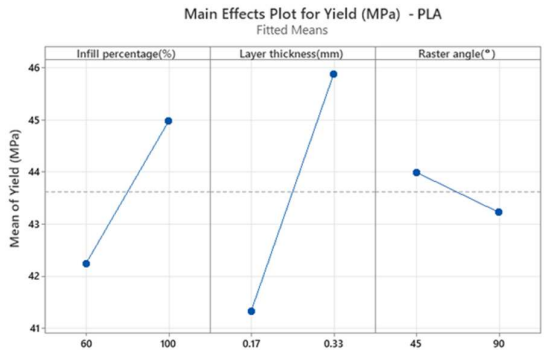

Fig.20. Main Effects Plot for Yield Ultimate Tensile Stress (MPa) PLA

The process under discussion has been demonstrated to facilitate the identification of factors that have a significant impact on outcomes by demonstrating how the mean response changes with each level of a factor.

In our study the main effects plot (Fig. 19 and Fig. 20) is employed to examine differences between level means for one or more factors, with a main effect occurring when different levels of a factor affect the response differently [15], [11]. The response mean for each factor level is graphically represented by a line in a main effects plot. When the line is not horizontal, it is indicative of a main effect, signifying that the different levels of the factor influence the response in a non-uniform manner.

The steeper the slope of the line, the more pronounced the main effect.

4. CONCLUSIONS

This paper presents contributions related to the integration of robotic arm in the additive manufacturing of materials using FDM process.

3D printing is a powerful manufacturing process which offers maximum flexibility in terms of the printed part, with virtually any designed geometry being achievable with good mechanical properties or good enough for the intended use.

Industrial robots and cobots alongside 3D printing are one the most prominent pillars of Industry 4.0 and present la largest growth potential. 3D printing has the ability to create intricate parts and robots have a large workspace the combination of the two pillars of Industry 4.0 are aimed to increase the capabilities of additive manufacturing and reduce the disparities compared to conventional material removal manufacturing process.

Most changes in the 3D printing industry are driven by technological advances, evolving consumer preferences and dynamic market conditions, but one trend remains constant: the development of customized products.

In general, 3D printing is a very good alternative to traditionally manufactured parts, which are usually CNC machined and assembled.

After the tests had been carried out, the research team concluded that:

- A stress-strain curve has been obtained. This is a graph which illustrates the relationship between the applied stress (i.e. the force per unit area) and the resultant strain (defined as the deformation of a material under stress).
- Ultimate Tensile Stress values for the PLA material were found to be higher by approximately 44% than the corresponding PETG material.

- The Ultimate Tensile Stress of PETG ranges from 29.38 to 40.54 MPa. The factors that define maximum values are "Infill Percentage"- 100%, "Raster Angle"- 90°, and last factor "Layer Thickness" (0.17mm and 0.33mm) do not influence the maximum values.
- Comparing with the Ultimate Tensile Stress of PETG, Ultimate tensile strength of PLA varies from 36.9 to 46.35 MPa. The factors that define maximum values are "Infill Percentage" - 60%,"Layer Thickness"- 0,33mm, and last factor "Raster Angle" (45° and 90°) do not have influence to this maximum values.
- The tensile strengths of both materials were found to be at their lowest when the 3D printing parameters were set to 60% for 'Infill Percentage', 45° for 'Raster Angle', and 0.17 mm for 'Layer Thickness'.
- Following a thorough examination of failure mode of specimens robot printed, can be observed from the elongation of the fibers in the fracture section subsequent conclusion the behavior of PETG is more ductile than PLA material a conclusion that is further validated by the results obtained through conventional 3D printing methodologies.

Once the process conditions and parameters involved in the printing process that affect the quality of the product have been identified, future models can be optimized.

In our future researches the intention is modify the factors (variables, current parameters) and adding other printing parameters (printing speed, nozzle and bad temperature and perimeter) to determine their influence that lead to improved results.

Another direction of research would be to apply all these properties of the material to a mechanical part (electrical box, screw, nut, gear wheel) on a real scale, test and measure it, and attempt to simulate these behaviors using finite element analysis software.

Also, for further research we suggest testing other composite materials.

This research was funded by National Research Grants - ARUT, Technical University "Gheorghe Asachi" of Iasi, Romania: GnaC2023_269.

5. REFERENCES

[1] Grand View Research, *Additive Manufacturing Market Size & Trends,* https://www.grandviewresearch.com/industry-analysis/additive-manufacturing-market, Accessed 2025.

[2] Edutanu, F.-D., Dumitraș, C. G., Grigoruță (Bișoc), C., *A Systematic Review of the Principles Used in Industry 5.0*, RECENT J. (2024), 74:192-200, https://doi.org/10.31926/RECENT.2024.74.192

[3] Research Prusa, *PETG*, https://help.prusa3d.com/article/petg_2059, Accessed 2025

[4] 3DKORDO, *Filament Everfil PETG*, https://3dkordo.eu/en/, 29 11 2024. [Online]. Available: https://3dkordo.eu/en/product/filament-everfil-petg-s10-diam-175mm-color-nevy-blue-weight-100kg-netto. [Accessed 02 2025]

[5] 3DKORDO, *Filament Everfil PLA*, https://3dkordo.eu/en/o-firmie, 29 11 2024. [Online]. Available: https://3dkordo.eu/en/product/filament-everfil-pla-n01-diam-175mm-color-black-weight-100kg-netto. [Accessed 01 2025].

[6] Ultimaker B.V., *How to 3D print with PLA and which materials to choose*, https://ultimaker.com/learn/how-to-3d-print-with-pla-and-which-materials-to-choose/,[Accessed 2025]

[7] ASTM International, "ASTM International," 07 2022. [Online]. Available: https://store.astm.org/d0638-14.html. [Accessed 02 2025].

[8] Paduraru, E., et al, *Research on Additive Technique Parameter Optimization for Robotic Gripper Construction*, Machines, 2023.

[9] Bharat, N. et al, *Influence of 3D Printing FDM Process Parameters on Compressive Strength of PLA/Carbon Fiber Composites: ANOVA and Backpropagation Neural Network Approach*, Journal of Materials Engineering and Performance, 2025.

[10] Hopcroft, M. A., Nix, W. D., Kenny, T. W., *What is the Young's Modulus of Silicon?,* Journal of Microelectromechanical Systems, vol. 19, no. 2, pp. 229-238, 2010.

[11] Minitab LLC, *Interpret the key results for Analyze Factorial Design*,

https://support.minitab.com/en-us/minitab/help-and-how-to/statistical-modeling/doe/how-to/factorial/analyze-factorial-design/interpret-the-results/key-results/?SID=128050, 2025
[12] Severino, P., et al, *Optimizing SLN and NLC by 22 full factorial design: Effect of homogenization technique*, Materials Science and Engineering, vol. 32, no. 6, pp. 1375-1379, 2012.
[13] Sedgwick, P., *What is a factorial study design?*, British Medical Journal, vol. 349, 2014.
[14] Kang, Jacob & Chia, Pei Zhi & Silva, Arlindo & Koronis, Georgios, *Exploring the Use of a Full Factorial Design of Experiment to Study Design Briefs for Creative Ideation*, Conference ASME 2018 International Design Engineering Technical Conferences and Computers and Information in Engineering Conference, Quebec, Canada, 2018.
[15] Antonio F. N., et al, *Use of Factorial Designs and the Response Surface Methodology to Optimize a Heat Staking Process*, Experimental Techniques, vol. 42, no. 3, 2018.
[16] Bingol, D., Tekin, N., Alkan, M., *Brilliant Yellow dye adsorption onto sepiolite using a full factorial design*, Applied Clay Science, vol. 50, no. 3, pp. 315-321, 2010.

Optimizarea procesului de imprimare 3D cu ajutorul unui braț robotic pentru îmbunătățirea proprietăților mecanice ale pieselor

Rezumat: Obiectivul prezentului studiu este de a analiza parametrii utilizați în procesul de imprimare 3D asistată de robot. Acești parametri analizați includ aspecte precum procentul densitatii de umplere, inaltimea stratului și unghiul de printare. După procesul robotizat de imprimare 3D, epruvetele sunt testate folosind standardul D638-14 într-o mașină de testare la tracțiune, unde se va aplica o forță axială crescândă epruvetei, de obicei până la rupere, iar variațiile rezultate vor fi documentate. Curba tensiune/deformare generată va demonstra modul în care materialul reacționează la forțele aplicate. Pentru imprimarea 3D robotizată cu materiale PLA și PETG, în timpul experimentelor efectuate, s-a constatat că valorile rezistentei la tractiune pentru materialul PLA sunt mai mari decât pentru materialul PETG.
Cuvinte cheie: Robot, Imprimare 3D, Rezistenta la tractiune, PETG, PLA.

Florin-Daniel EDUTANU, Ph.D Student, Faculty of Machines Manufacturing and Industrial Management; "Gheorghe Asachi" Technical University of Iasi, florin daniel.edutanu@student.tuiasi.ro, 0742040030.
Dragos-Florin CHITARIU, PhD Associate Professor, Faculty of Machines Manufacturing and Industrial Management; "Gheorghe Asachi" Technical University of Iasi, 700050 Iasi, Romania, dragos-florin.chitariu@academic.tuiasi.ro, 0741269491, Academy of Romanian Scientists, Ilfov 3, 050044 Bucharest, Romania.
Emilian PADURARU PhD Associate Professor, Faculty of Machines Manufacturing and Industrial Management; "Gheorghe Asachi" Technical University of Iasi, 700050 Iasi, Romania, emilian.paduraru@academic.tuiasi.ro, 0753159856.
Florin CHIFAN PhD Associate Professor, Faculty of Machines Manufacturing and Industrial Management; "Gheorghe Asachi" Technical University of Iasi, 700050 Iasi, Romania, florin.chifan@academic.tuiasi.ro, 0743068177.
Neculai-Eduard BUMBU PhD Associate Professor, Faculty of Machines Manufacturing and Industrial Management; "Gheorghe Asachi" Technical University of Iasi, 700050 Iasi, Romania, neculai-eduard.bumbu@academic.tuiasi.ro, 0755236692.
Mariana CIORAP Associate Professor, Faculty of Machines Manufacturing and Industrial Management; "Gheorghe Asachi" Technical University of Iasi, 700050 Iasi, Romania, mariana.ciorap@academic.tuiasi.ro, 0744787230.
Cătălin Gabriel DUMITRAȘ PhD Associate Professor, Faculty of Machines Manufacturing and Industrial Management; "Gheorghe Asachi" Technical University of Iasi, 700050 Iasi, Romania, catalin-gabriel.dumitras@academic.tuiasi.ro, 0740243158.